



Azo-hydrizo conversion via [1,5]-hydrogen shifts. A combined experimental and theoretical study

Edikarlos M. Brasil^a, Rosivaldo S. Borges^a, Oscar A.S. Romero^{a,*}, Claudio N. Alves^a, Jose A. Sáez^b, Luis R. Domingo^{b,*}

^a Departamento de Química, Instituto de Ciências Exatas e Naturais, Universidade Federal do Pará, CP 11101, 66075-110, Belém, PA, Brazil

^b Departamento de Química Orgánica, Universidad de Valencia, Dr. Moliner 50, 46100 Burjassot, Valencia, Spain

ARTICLE INFO

Article history:

Received 5 April 2012

Received in revised form 1 June 2012

Accepted 5 June 2012

Available online 12 June 2012

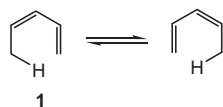
ABSTRACT

Azoalkenes **6e**, **6g**, **6h**, and **8c** underwent an easy azo-hydrizo conversion via a [1,5]-hydrogen shift yielding α,β -unsaturated hydrazones. The isomerization products were characterized through spectroscopic and spectrometric techniques. In order to understand the nature of the mechanism of these [1,5]-hydrogen shifts, the transition state structures of the reactions were theoretically studied at the B3LYP/6-31G(d,p) level. Substitution effects in the propenylazo system on the kinetic and thermodynamic parameters were analyzed. An electron localization function (ELF) analysis of the electronic structure of the transition state structure associated with the azo-hydrizo conversion of the simplest 1-azopropene **6a** indicates that these [1,5]-hydrogen shifts have a two-stage one-step mechanism via *pseudoradical* transition states, in which a formal hydrogen atom is transferred. This finding allows us to reject the pericyclic reaction model for these [1,5]-hydrogen shift reactions.

© 2012 Elsevier Ltd. All rights reserved.

1. Introduction

The [1,5]-hydrogen shift (15HS) reaction was first described by Wolinsky¹ when he observed a possible hydrogen shift in *cis*-1,3-pentadiene **1** and paid attention to its reaction mechanism (see Scheme 1). This reaction, classified within the pericyclic reaction model as a [1,5]-sigmatropic reaction, was one of the examples employed by R.B. Woodward and R. Hoffmann² to establish their well known conservation of orbital symmetry theory, further supported by the analysis of the first order kinetic isotopic effects (KIEs) made by Roth and König.^{3,4} Since then, the 15HS reaction has become part of the organic chemist toolbox as an alternative path to new synthetic methods.^{5–11}

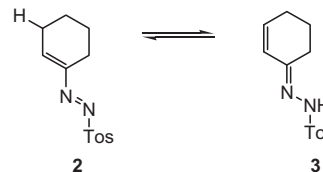


Scheme 1.

Although excellent theoretical studies involving [1,5]-sigmatropic reactions have been carried out, most of them

involve the *cis*-1,3-pentadiene system.^{12–15} Studies at B3LYP/6-31G(d) level of the 15HS reaction of *cis*-1,3-pentadiene **1**^{16–18} (see Scheme 1) concluded that this reaction takes place through a concerted transition state (TS), which is 32.9 kcal/mol higher than *trans*-1,3-pentadiene,¹⁸ a value close to that obtained through ¹H NMR experiments.³

Only few studies about 15HS reactions in heterodienic systems ($-\text{CH}_2-\text{C}=\text{C}-\text{X}=\text{Y}$; X=C, N and/or Y=N, O) have been reported.^{18–21} The azo-hydrizo conversion of 1-tosylazocyclohexene **2** into the tautomer cyclohex-2-enone tosylhydrazone **3** was reported by Dondoni et al. (Scheme 2).²² According to Dondoni, this azo-hydrizo conversion can take place in absence of a catalyst, but the polarity of the solvent has a low effect on the reaction rate.²²

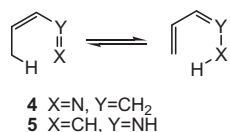


Scheme 2. Azo-hydrizo conversion of 1-tosylazocyclohexene **2**.

The 15HS reactions of several substituted 1,3-pentadiene and *aza*-1,3-pentadiene systems were studied by Saettel et al. using density functional theory (DFT) methods at B3LYP/6-31G(d) level

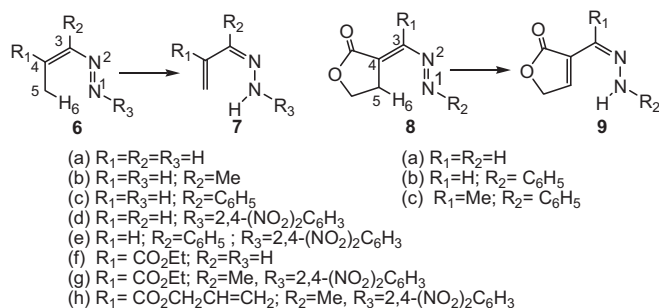
* Corresponding authors. E-mail address: domingo@utopia.uv.es (L.R. Domingo).

(see Scheme 3).¹⁸ For these 15HS reactions, which were classified as sigmatropic shifts within the pericyclic reaction model, the substitution effects on the activation energy were analyzed. The authors observed that the decrease of the electron density of the π system destabilizes the aromatic TS and increases the activation energy and vice versa. The activation energies computed for the 15HS reaction of *cis*-but-2-en-1-imine **4** and *cis*-*N*-methylenprop-1-en-1-amine **5**, 25.5 and 32.3 kcal/mol, respectively (see Scheme 3), were lower than that for *cis*-penta-1,3-diene **1**.¹⁸ On the other hand, the isomerization of **4** is exothermic by -3.7 kcal/mol, while for **5** is endothermic by 2.8 kcal/mol.



Scheme 3.

Herein, we report a combined experimental and theoretical approach to azoalkene systems undergoing azo-hydrazo conversions through 15HS processes. The synthesized azocompounds **6e**, **6g**, **6h**, and **8c** easily underwent an azo-hydrazo conversion into hydrazones **7e**, **7g**, **7h**, and **9c**, respectively (see Scheme 4). DFT calculations of the 15HS reactions of azoalkenes **6a–g** and **8a–c** to yield the corresponding hydrazones **7a–g** and **9a–c** were performed in order to establish their mechanism and disclose the substitution effect on the propenylazo moiety. The electron localization function (ELF) of the structures involved in the reaction path associated with the isomerization of the simplest azopropene **6a** was analyzed in order to characterize the electronic reorganization along the 15HS reaction and to establish the mechanism of this azo-hydrazo conversion.



Scheme 4.

2. Results and comments

First, experimental results of the conversion of azoalkenes **6e**, **6g**, **6h**, and **8c** into α,β -unsaturated hydrazones **7e**, **7g**, **7h**, and **9c** will be analyzed. Then, a DFT study of the mechanism of these 15HS reactions will be done, including a discussion about the influence of the propenylazo substituents on the kinetic and thermodynamic data. Finally, an ELF analysis of the structures along the IRC of the reaction of azoalkene **6a** will be carried out in order to understand the electronic reorganization along the 15HS reaction.

2.1. Experimental results

Azoalkenes **6e**, **6g**, and **6h** were generated through dehydrohalogenation of the corresponding 2,4-dinitrophenyl hydrazones by stirring them in dichloromethane with anhydrous sodium carbonate at room temperature or heating (see Scheme S1

in Supplementary Data). Azoalkene **8c** was obtained by van Alphen's method from its bromo derivative (see Section b in Supplementary Data). Refluxing azoalkene **6e** and indene under nitrogen for 20 h trying to obtain their cycloadduct left, after solvent removal, **7e** as orange crystals as the only product.

Likewise, attempting to obtain the intramolecular Diels–Alder cycloadduct from azoalkene **6g** by refluxing it in dry toluene under nitrogen for 18 h, yielded an orange gum after solvent removal. Treating this gum with ether to induce crystallization gave rise to yellow crystals in quantitative yield after 15 h, which were identified as compound **7g**.

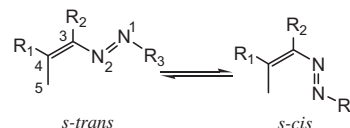
Again, stirring at room temperature azoalkene **6h** and butylvinyl ether for 24 h trying to obtain its cycloadduct, yielded an orange gum after solvent removal, which turned into yellow crystals characterized as **7h** upon purification procedures. Therefore, in **6e**, **6g**, and **6h** reactions, their corresponding 15HS products were obtained rather than the expected cycloadducts. This fact indicates that the 15HS process is favored over the cycloaddition reaction in these azoalkenes.

Starting from 3-acetyl-3-bromodihydrofuran-2(3*H*)-one, azoalkene **8c** was obtained as bright red crystals using van Alphen's method.²³ Upon attempting to recrystallize **8c** from ether–hexane and warming (39 °C), the red solution turned yellow, making it possible to quantitatively isolate a solid, identified as **9c**, by filtration. Hence, **6e**, **6g**, **6h**, and **8c** azoalkenes easily experienced a 15HS reaction to yield the corresponding hydrazo compounds **7e**, **7g**, **7h**, and **9c** without catalyst by heating them in solvent.

2.2. DFT study of the [1,5]-hydrogen shift at azoalkenes **6** and **8**

In order to understand the mechanism of the 15HS reactions of azoalkenes **6** and **8** to afford α,β -unsaturated hydrazones **7** and **9**, respectively, the corresponding reactions were studied using DFT methods at the B3LYP/6-31G(d,p) level (see Scheme 4). Analysis of the stationary points found along the potential energy surface (PES) indicates that the hydrogen shift from the donor C5 carbon to the acceptor N1 nitrogen of these azoalkenes takes place through a two-stage one-step mechanism.²⁴

The azoalkene N1=N2–C3=C4 framework can adopt a *s-trans* or *s-cis* conformation (see Scheme 5). The *s-trans* conformation of azoalkene **6a** is 4.8 kcal/mol more stable than the *s-cis* one, but the last conformation is required for the reaction to take place. Presence of a phenyl group at C3 (R₂=C₆H₅) in azoalkene **6c** does not modify this relative energy, 4.2 kcal/mol, due to the twist of the phenyl ring relative to the N1=N2–C3=C4 system, 50.4°.



Scheme 5.

The activation energies associated with the 15HS reactions of these azoalkenes range from 15.7 (**TS6c**) to 22.3 kcal/mol (**TS8b**) (see Table 1) (activation energies relative to the *s-cis* conformations are given). These energy barriers are lower than those for (*Z*)-but-2-en-1-imine **4** and (*Z*)-*N*-methylenprop-1-en-1-amine **5**, 25.5 kcal/mol and 32.3 kcal/mol, respectively.¹⁸ All processes are exothermic, ranging from -4.4 (**6f**) to -16.9 (**6e**) kcal/mol.

An analysis of the energy results given in Table 1 indicates that the effect of the substituents at N1, C3, and C4 (see Scheme 4), is

Table 1

Relative^a energies (ΔE) in gas phase and in DCM, and relative enthalpies (ΔH), entropies (ΔS), and free energies (ΔG), computed^b at 298.1 K and 1 atm associated with the [1,5]-hydrogen shifts on azoalkenes **6** and **8**

	ΔE_{vacuo} (kcal/mol)	ΔE_{solv} (kcal/mol)	ΔH (kcal/mol)	ΔS (cal/mol K)	ΔG (kcal/mol)
TS6a	19.0	20.1	16.7	-2.9	17.5
TS6b	19.7	20.9	16.7	-5.7	18.4
TS6c	15.7	17.5	14.0	2.7	13.2
TS6d	20.3	21.4	17.2	-7.8	19.6
TS6e	18.1	19.4	14.9	-7.0	17.0
TS6f	20.0	21.5	17.0	-4.6	18.4
TS6g	21.9	21.9	18.8	-6.7	20.9
TS8a	18.4	19.6	15.3	-5.7	17.0
TS8b	22.3	23.5	19.0	-6.0	20.8
TS8c	20.8	21.5	17.5	-5.3	19.0
7a	-6.6	-8.0	-5.3	-1.1	-5.6
7b	-5.8	-6.6	-5.1	2.2	-4.5
7c	-8.8	-10.1	-6.9	-6.6	-8.9
7d	-14.5	-15.0	-13.6	4.4	-12.3
7e	-16.9	-17.8	-16.2	3.2	-15.2
7f	-4.4	-5.5	-3.8	0.6	-3.6
7g	-6.5	-9.7	-6.0	0.3	-5.9
9a	-11.1	-13.1	-10.7	1.7	-10.1
9b	-5.9	-7.7	-5.6	1.6	-5.2
9c	-5.3	-7.3	-5.2	1.6	-4.7

^a Relative to *s-cis* conformation of azoalkenes **6** and **8**.

^b Frequencies scaled by 0.96.

moderate over the energy barriers, since different substitution patterns render relatively small energy differences (note that the 15HS activation energy difference between **TS6c** and **TS8b** at Table 1 is 6.6 kcal/mol). Thus, a good example can be found when comparing the 15HS reactions of **6d** and **6e**, where changing R_2 at C3 from a hydrogen to a phenyl group yields a decrease of ca. 2.3 kcal/mol in their reaction barrier. Again, changing R_2 from a hydrogen **8b** to a methyl group **8c**, results in a decrease of ca. 1.5 kcal/mol. Finally, the difference between **6b** and **6c** is their substituent at C3 (methyl and phenyl, respectively) and their energy barriers differ by ca. 2 kcal/mol. Therefore, the introduction of electron-releasing groups at the C3 carbon of the azoalkene moiety results in a slight reduction of the 15HS energy barrier.

The substitution effect on N1 is more difficult to rationalize, since changing the substitution at N1 from a hydrogen **6a** to an electron-withdrawing 2,4-dinitrophenyl group **6d** increases the energy barrier by ca. 1.3 kcal/mol, and the change at N1 in **8** moiety from hydrogen **8a** to a phenyl group **8b**, increases the barrier by 4 kcal/mol. Therefore, 2,4-dinitrophenyl and phenyl groups, although having different electronic behaviors, render the same qualitative effect on the 15HS energy barriers. Then, the electronic delocalization (present at both 2,4-dinitrophenyl and phenyl groups) may be the prevalent effect appearing in this position at the azoalkene moiety.

The inclusion of solvent effects of dichloromethane (DCM) through single point PCM calculations over the gas phase B3LYP/6-31G(d,p) geometries does not modify the gas phase B3LYP/6-31G(d,p) energies (see Table 1). In general, the activation energies in DCM increase only between 0.7 and 1.7 kcal/mol, due to a better solvation of azoalkenes than TSs. Similar results are observed in [3+2] cycloadditions with non-polar character, where dipoles are better solvated than TSs.²⁵

Inclusion of thermal corrections and entropies to electronic energies decreases the activation free energies between 0.8 and 2.5 kcal/mol (see Table 1). This effect is mainly due to the low activation entropies associated with these unimolecular processes, between -2.9 and -7.8 kcal/mol K. Thus, the activation free energies associated with the experimental reactions are: 17.0 (**TS6e**), 20.9 (**TS6g**), and 19.0 (**TS8c**) kcal/mol, while the reaction free

energies are: -15.2 (**7e**), -5.9 (**7g**), and -4.7 (**9c**) kcal/mol. These kinetic and thermodynamic data are in reasonable agreement with the experimental results, where a complete transformation upon moderate heating is observed (dichloromethane or toluene reflux).

Geometries of the optimized TSs associated with the 15HS reactions present quite similar N1-H6 and H6-C5 forming- and breaking-bond distances, ranging from 1.345 to 1.402 Å (N1-H6) and 1.300 to 1.344 Å (H6-C5), respectively (see Figs. 1 and 2). Looking at N1-H6 forming- and H6-C5 breaking bonds at the TSs of both **6** and **8** 15HS reactions, it can be seen that these processes are slightly asynchronous, as N-H distances are always slightly higher than C-H ones. Note that, in methylamine, the lengths of the N-H bonds, 1.017 Å, are shorter than the C-H ones, 1.095 Å, at the same computational level.

The extent of breaking- and forming-bonds at the TSs involved in these 15HS reactions was analyzed using the Wiberg bond order (BO) values (see Table 2).²⁶ In all studied cases, the N1-H6 forming-

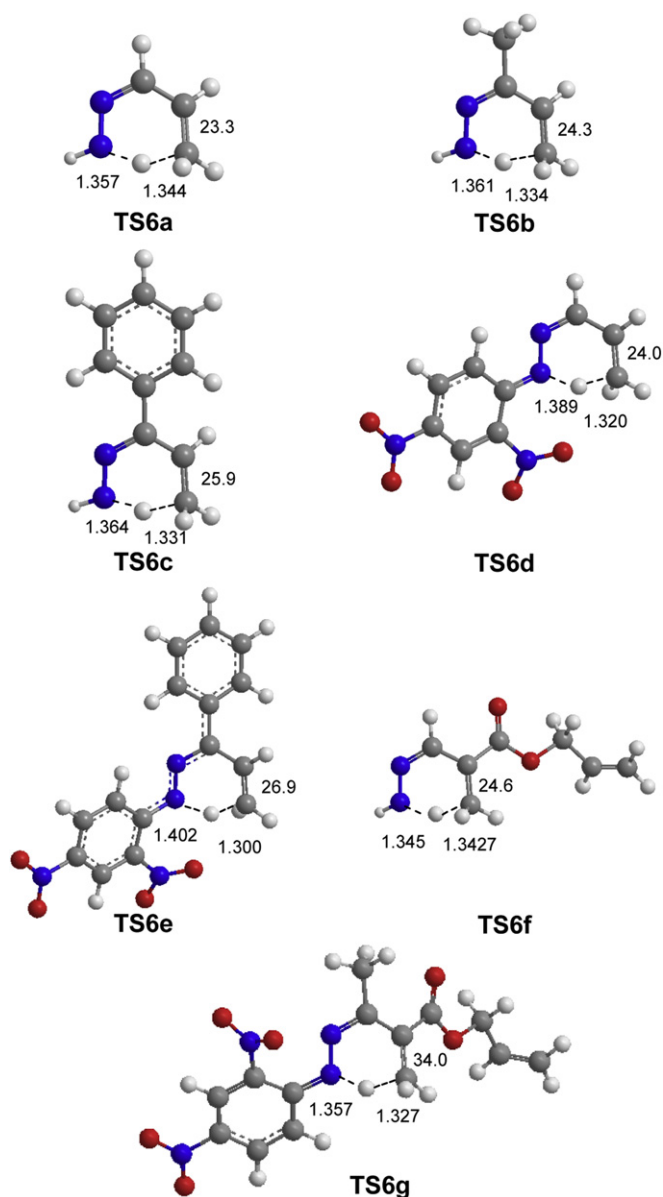


Fig. 1. Geometries of the transition states **TS6a–g** associated with the [1,5]-hydrogen shifts of azoalkenes **6a–g**. The distances are given in Å, while the H6-C5-C4-C3 dihedral angles are given in degrees.

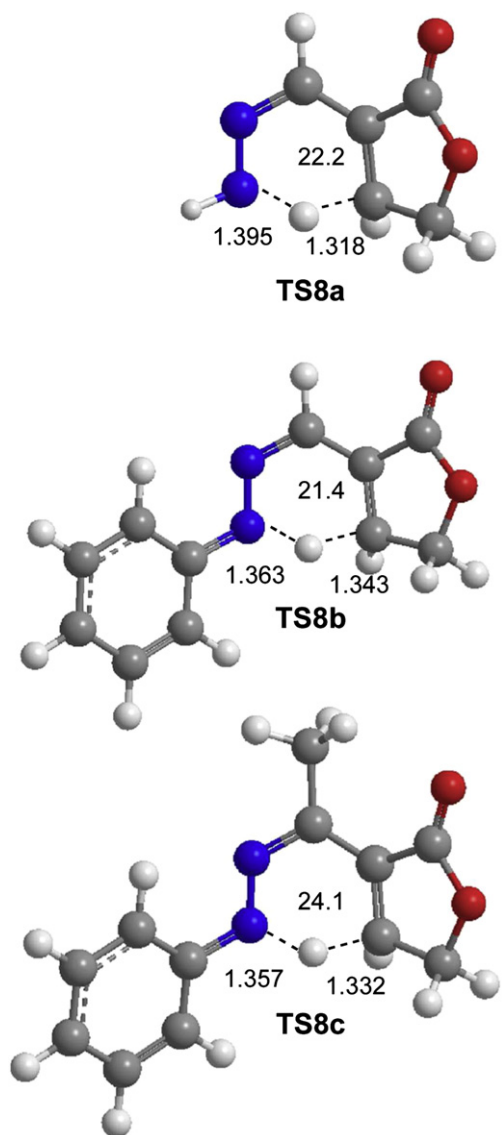


Fig. 2. Geometries of the transition states **TS8a–c** associated with the [1,5]-hydrogen shifts of azoalkenes **8a–c**. The distances are given in Å, while the H6–C5–C4–C3 dihedral angles are given in degrees.

Table 2

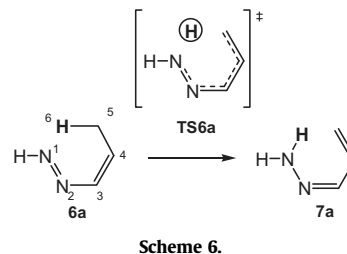
Wiberg bond orders (BOs) at the TSs associated with the [1,5]-hydrogen shifts on azoalkenes **6** and **8**

	BO(C5–H6)	BO(N1–H6)
TS1a	0.46	0.38
TS1b	0.47	0.38
TS1c	0.47	0.37
TS1d	0.47	0.33
TS1e	0.48	0.31
TS1f	0.46	0.39
TS1g	0.46	0.36
TS3a	0.48	0.36
TS3b	0.45	0.36
TS3c	0.45	0.36

bond has a lower BO value, ranging from 0.31 to 0.39, when compared to the C5–H6 breaking bond, whose BO ranges from 0.45 to 0.48. Thus, these values indicate that the H6–C5 breaking-bond process is more advanced than the N1–H6 forming-bond. In addition, the narrow range of the C5–H6 and N1–H6 BO values, indicates that the substitution on the propenyldiazene system of azoalkenes **6** and **8** does not produce an appreciable effect on the molecular mechanism of these 15HS reactions.

2.3. ELF topological analysis of the bond-breaking and bond-formation along the [1,5]-hydrogen shift on 1-((Z)-prop-1-enyl)diazene **6a**

The topology of the ELF of some selected points along the 15HS reaction at the simplest azoalkene **6a** was studied to obtain additional information about the electron density reorganization in these reactions, and thus, to characterize the molecular mechanism of these 15HS reactions (see Scheme 6).²⁷ The populations of the most relevant valence basins, *N*, of these structures are listed in Table 3, where d1 stands for the C5–H6 distance and d2 for the N1–H6 one.



The electronic structure of azoalkene **6a**, point I, d1=2.41 and d2=1.09 Å, shows two disynaptic basins, V(C4,C5) and V(N2,C3), which integrate ca. 2 e each one, representing the corresponding single bonds. Also, two disynaptic basins appear, namely V(C3,C4) and V'(C3,C4), which integrate 1.90 and 1.64 e, respectively, and correspond to the C3–C4 double bond. Only one disynaptic basin V(N1–N2), with an electronic population of 2.27 e, is found in the N1=N2 region. Two monosynaptic basins are found at N1 and N2 nitrogen, respectively, V(N1) and V(N2), with an electronic population of 2.70 e and 2.75 e, respectively.

On going from azoalkene **6a** to **TS6a**, the first relevant change takes place at point III, d1=1.10 and d2=1.93 Å, where the two disynaptic basins V(C3,C4) and V'(C3,C4) merge into only one disynaptic basin V(C3,C4), which integrates ca. 3.50 e. Along the IRC, the electronic population of V(C3,C4) decreases slowly to reach an electronic population of 2.26 e at the hydrazoalkene **7a**.

At point IV, d1=1.32 and d2=1.39 Å, only changes of electron population of the basins are observed. Thus, while the electronic

Table 3

ELF valence basin populations of selected geometries from the IRC of [1,5]-hydrogen shift of azoalkene **6a**, together with the C5–H6 (d1) and N1–H6 (d2) distances and BOs characterizing each point

	I	II	III	IV	V	VI	VII	VIII	IX	X
	6a	TS6a				7a				
d1	1.093	1.099	1.100	1.322	1.357	1.481	1.525	1.649	1.805	2.456
d2	2.415	1.952	1.925	1.392	1.354	1.222	1.177	1.075	1.035	1.023
BO(C5–H6)	0.91	0.86	0.85	0.50	0.46	0.30	0.25	0.14	0.08	0.01
BO(N1–H6)	0.01	0.05	0.05	0.35	0.39	0.53	0.58	0.68	0.75	0.82
V(N1,N2)	2.27	2.26	2.23	1.85	1.79	1.71	1.69	1.64	1.60	1.45
V(N2,C3)	2.03	2.13	2.14	2.53	2.57	2.66	2.73	2.93	3.07	3.22
V(C3,C4)	1.90	1.96	3.50	3.02	2.98	2.81	2.75	2.50	2.31	2.26
V'(C3,C4)	1.64	1.57								
V(C4,C5)	2.06	2.05	2.03	2.37	2.43	2.63	2.68	3.35	1.78	1.78
V'(C4,C5)									1.65	1.68
V(N1)	2.75	2.83	2.84	3.06	3.04	2.11	2.04	1.98	1.95	1.99
V(N2)	2.70	2.65	2.66	2.86	2.89	2.85	2.84	2.83	2.74	2.79
V(N1,H6)						0.81	1.75	1.88	1.99	2.04
V(C5,H6)	2.01	1.94	1.93	1.66						
V(C5)					0.76	0.70	0.66			
V(H6)					0.84	0.88				

population of the disynaptic basin $V(C3,C4)$ decreases to 3.02 e, the disynaptic basins $V(C4,C5)$ and $V(N2,C3)$ increase to 2.37 e and 2.53 e, respectively. On the other hand, the disynaptic basin $V(C5,H6)$ integrates 1.66 e.

At **TS6a**, point V, $d1=1.36$ and $d2=1.35$ Å, the most relevant changes of the electronic structure of azoalkene **6a** along the IRC are observed. While the disynaptic basin $V(C5,H6)$ disappears, indicating the complete C5–H6 breaking bond, two new monosynaptic basins $V(C5)$ and $V(H6)$, which integrate 0.76 e and 0.84 e, respectively, are created. These monosynaptic basins point to a homolytic C5–H6 breaking bond. Consequently, the ELF topology of **TS6a** indicates that the electronic structure of this TS corresponds with a *pseudodiradical* species,^{28–30} in which ca. 1 e is located at the donor C5 carbon atom and another one at the transferring H6 hydrogen atom. **TS6a** divides the two stages of this 15HS reaction; while the C5–H6 bond breaks before **TS6a**, the N1–H6 bond-formation takes place after passing **TS6a**. This representation makes it possible to discard a simultaneous bonding reorganization at the six-membered TS, as proposed by the pericyclic reaction model.

At point VI ($d1=1.48$ and $d2=1.22$ Å), while the electron population of the monosynaptic basin $V(N1)$ decreases by 0.93 e, a new disynaptic basin $V(N1,H6)$, with an electron population of 0.81 e, emerges. This basin is associated with the formation of the new N1–H6 bond. Note that at this point, the $V(C5)$ and $V(H6)$ monosynaptic basins coexist. At point VII ($d1=1.53$ and $d2=1.18$ Å), the monosynaptic basin $V(H6)$ disappears, the corresponding electron density being collected in the disynaptic basin $V(N1,C6)$, which reaches an electron density of 1.75 e.

At point VIII, $d1=1.65$ and $d2=1.08$ Å, the monosynaptic basin $V(C5)$ disappears while the electron population of the disynaptic basin $V(C4,C5)$ reaches 3.35 e. Finally, at point IX, $d1=1.81$ and $d2=1.04$ Å, the disynaptic basin $V(C4,C5)$ disassociates into two disynaptic basins $V(C4,C5)$ and $V'(C4,C5)$, which integrate 1.78 e and 1.65 e, respectively. They are associated with the C4=C5 double bond present at the hydrazoalkene **7a**. Finally, the more relevant features of the hydrazoalkene **7a** are the two disynaptic basins $V(C4,C5)$ and $V'(C4,C5)$, which integrate 1.78 and 1.68 e, respectively, the disynaptic basins $V(C3,C4)$ and $V(N2,C3)$, which integrate 2.26 e and 3.22 e, respectively, and two monosynaptic basins $V(N1)$ and $V(N2)$, which integrate 1.99 and 2.79 e, respectively. ELF analysis of the hydrazoalkene **7a** displays a conjugated N2–C3–C4–C5 system, strongly polarized toward the N2 nitrogen atom.

From this ELF analysis it can be concluded that along the 15HS reaction of azoalkene **6a**, the most significant changes of the breaking- and forming-bond processes take place at two well characterized points of the IRC: (i) at point V, $d1=1.36$ and $d2=1.35$ Å, which corresponds to **TS6a**, where the disynaptic basin $V(C5,H6)$ disappears, indicating that the C5–H6 bond has been broken, and two new monosynaptic basins, $V(C5)$ and $V(H6)$, appear. This behavior points to an initial homolytic C5–H6 breaking bond with formation of a *pseudodiradical* species and (ii) at point VI, $d1=1.48$ Å and $d2=1.22$ Å, where a new disynaptic basin $V(N1,H6)$, associated with the formation of the new N1–H6 bond, emerges. These results point to a non-synchronous C5–H6 bond-breaking and N1–H6 bond-formation process, because they take place before and after passing the TS, respectively. Consequently, **TS6a** divides the two-stages of the reaction.³⁰ Interestingly, the ELF description of **TS6a** corresponds to a *pseudodiradical* structure, with an appreciable electron density located at the C5 and H6 atoms, 0.76 e and 0.84 e, respectively. Therefore, this 15HS reaction must be described as a hydrogen atom transfer process from the donor C5 carbon to the acceptor N1 nitrogen, instead of a sigmatropic reaction defined within the pericyclic reaction model, in which the H6 hydrogen would be transferred by a concerted breaking- and

forming-bond process between the C5 and N1 centers, through a cyclic six-membered TS.

3. Conclusions

α,β -Unsaturated hydrazones **7e**, **7g**, **7h**, and **9c** have been obtained from their azoalkene precursors **6e**, **6g**, **6h**, and **8c** with excellent yields via a 15HS reaction, just heating them without catalyst. DFT calculations have been performed in order to rationalize the mechanism of these 15HS reactions and to disclose the substitution effects on the kinetic and thermodynamic parameters of the process. These reactions take place through a two-stage one-step mechanism. Activation energies range from 15.7 to 22.3 kcal/mol, being 19.0 kcal/mol for the simplest azoalkene **6a**. The largest acceleration is observed when C3 is substituted by a phenyl group (**6c**). All these reactions are exothermic. Inclusion of solvent effects increases the activation energies slightly due to a stronger solvation of azoalkenes than of the corresponding non-polar TSs.

ELF analysis of some relevant points along the IRC from the simplest azoalkene **6a** to the α,β -unsaturated hydrazone **7a** allows for the characterization of the electron-reorganization along this 15HS reaction. The most relevant changes take place at **TS6a**. ELF analysis of the TS evidences that the reaction takes place through a hydrogen atom transfer process from the donor C5 to the acceptor N1 via a *pseudodiradical* species, which is achieved by a homolytic C–H breaking bond. Thus, while the C–H bond has already been broken at **TS6a**, the N–H bond has not been formed yet.

The ELF representation for the electron-reorganization along these [1,5]-hydrogen shifts, which is characterized as a *hydrogen atom migration between the two extremes of a azoalkene*, allows us to reject a sigmatropic rearrangement process, defined within the pericyclic reaction model as a *reorganization of electrons during, which an atom or group attached by a σ bond migrate to the other terminus of a conjugate π -electron with a simultaneous shift of the π electrons*.³¹

Acknowledgements

The authors would like to thank CAPES and CNPq from the Brazilian Government and the Spanish Government (project CTQ2009-11027/BQU) for their financial support.

Supplementary data

Detailed procedures and full characterization of all synthetic products are provided along with computational methods used in the theoretical study. Supplementary data associated with this article can be found, in the online version, at <http://dx.doi.org/10.1016/j.tet.2012.06.013>.

References and notes

- Wolinsky, J.; Chollar, B.; Baird, M. D. *J. Am. Chem. Soc.* **1962**, *84*, 2775.
- Woodward, R. B.; Hoffmann, R. *J. Am. Chem. Soc.* **1965**, *87*, 2511.
- Roth, W. R.; König, J. *Liebigs Ann. Chem.* **1966**, *699*, 24.
- Roth, W. R.; König, J.; Stein, K. *Chem. Ber.* **1970**, *103*, 426.
- Hansson, T.; Sterner, O.; Wickberg, B. *J. Org. Chem.* **1992**, *57*, 3822.
- Feldman, K. S. *J. Am. Chem. Soc.* **1997**, *62*, 4983.
- Lenihan, B. D.; Shechter, H. *J. Org. Chem.* **1998**, *63*, 2086.
- Korth, H.-G.; Sustmann, R.; Lommes, P.; Paul, T.; Ernst, A.; de Groot, H.; Hughes, L.; Ingold, K. U. *J. Am. Chem. Soc.* **1994**, *116*, 2767.
- Diedrich, M. K.; Klärner, F.-G. *J. Am. Chem. Soc.* **1998**, *120*, 6212.
- Scott, A. I. *Angew. Chem., Int. Ed. Engl.* **1993**, *32*, 1223.
- Roessner, C. A.; Spencer, J. B.; Stolowich, N. J.; Wang, J.; Nayar, G. P.; Santander, P. J.; Pichon, C.; Min, C.; Holderman, M. T.; Scott, A. I. *Chem. Biol.* **1994**, *1*, 119.
- Hess, B. A., Jr.; Baldwin, J. E. *J. Org. Chem.* **2002**, *67*, 6025.
- Hayase, S.; Hrovat, D. A.; Borden, W. T. *J. Am. Chem. Soc.* **2004**, *126*, 10028.
- Doering, W. v. E.; Keliher, E. J.; Zhao, X. *J. Am. Chem. Soc.* **2004**, *126*, 14206.
- Alabugin, I. V.; Manoharan, M.; Breiner, B.; Lewis, F. D. *J. Am. Chem. Soc.* **2003**, *125*, 9329.

16. Alkorta, I.; Elguero, J. *J. Chem. Soc., Perkin Trans. 2* **1998**, 2497.
17. Jursic, B. S. *J. Mol. Struct. (Theochem)* **1998**, 423, 189.
18. Saettel, N. J.; Wiest, O. *J. Org. Chem.* **2000**, 65, 2331.
19. Radom, L.; Bouma, J. W. *J. Am. Chem. Soc.* **1979**, 101, 3487.
20. Skibo, B. E.; Xing, C. *Biochemistry* **2000**, 39, 10770.
21. Alajarin, M.; Sanchez-Andrada, P.; Lopez-Leonardo, C.; Alvarez, A. *J. Org. Chem.* **2005**, 70, 7617.
22. Dondoni, A.; Rossini, G.; Mossa, G.; Caglioti, L. *J. Chem. Soc. B* **1968**, 1404.
23. van Alphen, J. *Recl. Trav. Chim. Pays-Bas* **1945**, 64, 305.
24. Domingo, L. R.; Saéz, J. A.; Zaragoza, R. J.; Arnó, M. *J. Org. Chem.* **2008**, 73, 8791.
25. Benchouk, W.; Mekelleche, S. M.; Silvi, B.; Aurell, M. J.; Domingo, L. R. *J. Phys. Org. Chem.* **2011**, 24, 611.
26. Wiberg, K. B. *Tetrahedron* **1968**, 24, 1083.
27. Polo, V.; Andres, J.; Berski, S.; Domingo, L. R.; Silvi, B. *J. Phys. Chem. A* **2008**, 112, 7128.
28. In 1960 Errede et al. studied the high chemical reactivity of *p*-xylylene, which was attributed to its *pseudodiradical* character. They defined a *pseudodiradical* as a diamagnetic compound that behaves chemically as if were a diradical. Errede, L. A.; Hoyt, J. M.; Gregorian, R. S. *J. Am. Chem. Soc.* **1960**, 53, 5224.
29. Domingo, L. R.; Chamorro, E.; Perez, P. *Org. Biomol. Chem.* **2010**, 8, 5495.
30. Domingo, L. R.; Saez, J. A. *J. Org. Chem.* **2011**, 76, 373.
31. Carey, F. A.; Sundberg, R. J. *Advanced Organic Chemistry. Part A: Structure and Mechanisms*; Kluwer Academic/Plenum Publishers: New York, NY, 2000.